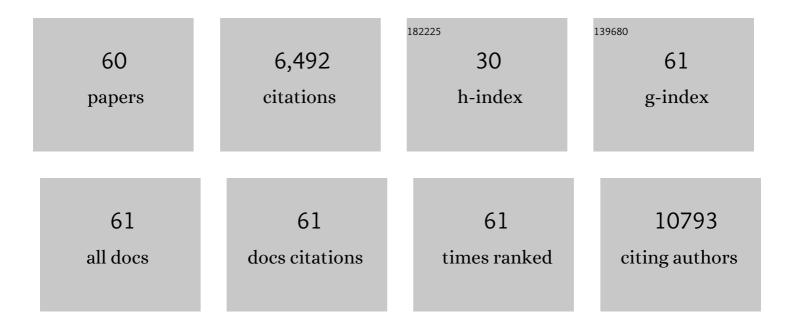
## List of Publications by Year in descending order

Source: https://exaly.com/author-pdf/3926911/publications.pdf Version: 2024-02-01



Χίνι Οιλνι

#	Article	lF	CITATIONS
1	Significant suppression of phonon transport in polar semiconductors owing to electron-phonon-induced dipole coupling: An effect of breaking centrosymmetry. Materials Today Physics, 2022, 22, 100598.	2.9	5
2	Confinement effect on thermopower of electrolytes. Materials Today Physics, 2022, 23, 100627.	2.9	4
3	Sol–Gel-Derived Biodegradable Er-Doped ZnO/Polyethylene Glycol Nanoparticles for Cell Imaging. ACS Applied Nano Materials, 2022, 5, 7103-7112.	2.4	7
4	Ionic thermoelectric materials for near ambient temperature energy harvesting. Applied Physics Letters, 2021, 118, .	1.5	40
5	Thermal conductivity modeling on highly disordered crystalline Y1â^' <i>x</i> Nb <i>x</i> O1.5+ <i>x</i> : Beyond the phonon scenario. Applied Physics Letters, 2021, 118, .	1.5	10
6	Phonon-engineered extreme thermal conductivity materials. Nature Materials, 2021, 20, 1188-1202.	13.3	254
7	Imaging the Néel vector switching in the monolayer antiferromagnet MnPSe3 with strain-controlled Ising order. Nature Nanotechnology, 2021, 16, 782-787.	15.6	70
8	Thermal conductance of nanostructured interfaces from Monte Carlo simulations with <i>ab initio</i> based phonon properties. Journal of Applied Physics, 2021, 129, .	1.1	4
9	High-temperature phonon transport properties of SnSe from machine-learning interatomic potential. Journal of Physics Condensed Matter, 2021, 33, 405401.	0.7	24
10	Radiative heat and momentum transfer from materials with broken symmetries: opinion. Optical Materials Express, 2021, 11, 3125.	1.6	18
11	Toward Optimal Heat Transfer of 2D–3D Heterostructures <i>via</i> van der Waals Binding Effects. ACS Applied Materials & Interfaces, 2021, 13, 46055-46064.	4.0	15
12	Machine learning for predicting thermal transport properties of solids. Materials Science and Engineering Reports, 2021, 146, 100642.	14.8	36
13	Thermally regenerative electrochemically cycled flow batteries with pH neutral electrolytes for harvesting low-grade heat. Physical Chemistry Chemical Physics, 2021, 23, 22501-22514.	1.3	27
14	Favorable Redox Thermodynamics of SrTi <sub>0.5</sub> Mn <sub>0.5</sub> O <sub>3â~î´</sub> in Solar Thermochemical Water Splitting. Chemistry of Materials, 2020, 32, 9335-9346.	3.2	42
15	Intrinsic nonreciprocal reflection and violation of Kirchhoff's law of radiation in planar type-I magnetic Weyl semimetal surfaces. Physical Review B, 2020, 102, .	1.1	69
16	Nanoparticle Mobility within Permanently Cross-Linked Polymer Networks. Macromolecules, 2020, 53, 4172-4184.	2.2	29
17	Accurate measurement of in-plane thermal conductivity of layered materials without metal film transducer using frequency domain thermoreflectance. Review of Scientific Instruments, 2020, 91, 064903.	0.6	29
18	Monitoring anharmonic phonon transport across interfaces in one-dimensional lattice chains. Physical Review E, 2020, 101, 022133.	0.8	8

#	Article	IF	CITATIONS
19	Correlations and incipient antiferromagnetic order within the linear Mn chains of metallic Ti4MnBi2. Physical Review B, 2020, 102, .	1.1	6
20	Giant thermopower of ionic gelatin near room temperature. Science, 2020, 368, 1091-1098.	6.0	382
21	Large nonreciprocal absorption and emission of radiation in type-I Weyl semimetals with time reversal symmetry breaking. Physical Review B, 2020, 101, .	1.1	84
22	Enhanced strength and self-healing properties of CA-Mg2/PVA IPN hydrogel used for shot-membrane waterproofing materials. Journal of Polymer Research, 2020, 27, 1.	1.2	9
23	Locust bean gum/gellan gum double-network hydrogels with superior self-healing and pH-driven shape-memory properties. Soft Matter, 2019, 15, 6171-6179.	1.2	44
24	Thermal conductivity modeling using machine learning potentials: application to crystalline and amorphous silicon. Materials Today Physics, 2019, 10, 100140.	2.9	48
25	Konjac glucomannan/kappa carrageenan interpenetrating network hydrogels with enhanced mechanical strength and excellent self-healing capability. Polymer, 2019, 184, 121913.	1.8	51
26	Diffused Lattice Vibration and Ultralow Thermal Conductivity in the Binary Ln–Nb–O Oxide System. Advanced Materials, 2019, 31, e1808222.	11.1	49
27	Preparation of konjac glucomannan–borax hydrogels with good self-healing property and pH-responsive behavior. Journal of Polymer Research, 2019, 26, 1.	1.2	19
28	Poly(lactic acid)–thermoplastic poly(ether)urethane composites synergistically reinforced and toughened with short carbon fibers for threeâ€dimensional printing. Journal of Applied Polymer Science, 2018, 135, 46483.	1.3	11
29	Highly efficient solar vapour generation via hierarchically nanostructured gels. Nature Nanotechnology, 2018, 13, 489-495.	15.6	1,356
30	Sol–gel solvothermal route to synthesize anatase/brookite/rutile TiO2 nanocomposites with highly photocatalytic activity. Journal of Sol-Gel Science and Technology, 2018, 85, 394-401.	1.1	20
31	A new elliptical-beam method based on time-domain thermoreflectance (TDTR) to measure the in-plane anisotropic thermal conductivity and its comparison with the beam-offset method. Review of Scientific Instruments, 2018, 89, 094902.	0.6	30
32	Tutorial: Time-domain thermoreflectance (TDTR) for thermal property characterization of bulk and thin film materials. Journal of Applied Physics, 2018, 124, .	1.1	197
33	Temperature effect on the phonon dispersion stability of zirconium by machine learning driven atomistic simulations. Physical Review B, 2018, 98, .	1.1	39
34	Three-dimensional anisotropic thermal conductivity tensor of single crystalline β-Ga2O3. Applied Physics Letters, 2018, 113, .	1.5	84
35	Design of End-to-End Assembly of Side-Grafted Nanorods in a Homopolymer Matrix. Macromolecules, 2018, 51, 4143-4157.	2.2	26
36	Thermal conductivity of polymers and polymer nanocomposites. Materials Science and Engineering Reports, 2018, 132, 1-22.	14.8	551

#	Article	IF	CITATIONS
37	Anisotropic thermal transport in van der Waals layered alloys WSe2(1- <i>x</i> )Te2 <i>x</i> . Applied Physics Letters, 2018, 112, .	1.5	32
38	<b>Anisotropic thermal transport in bulk hexagonal boron nitride</b> . Physical Review Materials, 2018, 2, .	0.9	73
39	Influence of nanoparticle size distribution on the thermal conductivity of particulate nanocomposites. Europhysics Letters, 2017, 117, 24001.	0.7	27
40	Synthesis of carbon modified TiO2 photocatalysts with high photocatalytic activity by a facile calcinations assisted solvothermal method. Journal of Materials Science: Materials in Electronics, 2017, 28, 10028-10034.	1.1	13
41	Tailoring the alignment of string-like nanoparticle assemblies in a functionalized polymer matrix via steady shear. RSC Advances, 2017, 7, 8898-8907.	1.7	4
42	Thermal conductivity modeling of hybrid organic-inorganic crystals and superlattices. Nano Energy, 2017, 41, 394-407.	8.2	32
43	Probing Anisotropic Thermal Conductivity of Transition Metal Dichalcogenides MX <sub>2</sub> (M =) Tj ETQq1	1 0,78431 11.1	.4 rgBT /Ov∈ 163
44	Time-domain thermoreflectance (TDTR) measurements of anisotropic thermal conductivity using a variable spot size approach. Review of Scientific Instruments, 2017, 88, 074901.	0.6	101
45	High-efficiency and magnetically separable nanocatalyst: β-cyclodextrin modified core–shell hybrid magnetic nanoparticles. Journal of Inclusion Phenomena and Macrocyclic Chemistry, 2017, 87, 45-51.	0.9	1
46	Anisotropic thermal conductivity of 4H and 6H silicon carbide measured using time-domain thermoreflectance. Materials Today Physics, 2017, 3, 70-75.	2.9	91
47	Super-stretchable borophene. Europhysics Letters, 2016, 116, 36001.	0.7	22
48	Lattice thermal conductivity of organic-inorganic hybrid perovskite CH3NH3PbI3. Applied Physics Letters, 2016, 108, .	1.5	97
49	Measurement Techniques for Thermal Conductivity and Interfacial Thermal Conductance of Bulk and Thin Film Materials. Journal of Electronic Packaging, Transactions of the ASME, 2016, 138, .	1.2	328
50	Photocatalytic Degradation of Dyes in Water Using TiO2/Hydroxyapatite Composites. Water, Air, and Soil Pollution, 2016, 227, 1.	1.1	8
51	Anisotropic Tuning of Graphite Thermal Conductivity by Lithium Intercalation. Journal of Physical Chemistry Letters, 2016, 7, 4744-4750.	2.1	69
52	A facile preparation of p <scp>H</scp> â€ŧemperature dual stimuliâ€ŧesponsive supramolecular hydrogel and its controllable drug release. Journal of Applied Polymer Science, 2016, 133, .	1.3	13
53	Anisotropic Thermal Transport in Organic–Inorganic Hybrid Crystal β-ZnTe(en)0.5. Journal of Physical Chemistry C, 2015, 119, 28300-28308.	1.5	16
54	The Vacancy Effect on Thermal Interface Resistance between Aluminum and Silicon by Molecular Dynamics. Materials Research Society Symposia Proceedings, 2015, 1753, 7.	0.1	1

#	Article	IF	CITATIONS
55	Crystallization, rheology and foam morphology of branched PLA prepared by novel type of chain extender. Macromolecular Research, 2015, 23, 231-236.	1.0	37
56	Tunable thermo-responsive supramolecular hydrogel: design, characterization, and drug release. Journal of Polymer Research, 2015, 22, 1.	1.2	6
57	Dielectric Mismatch Mediates Carrier Mobility in Organic-Intercalated Layered TiS <sub>2</sub> . Nano Letters, 2015, 15, 6302-6308.	4.5	62
58	Quantum spin Hall effect in two-dimensional transition metal dichalcogenides. Science, 2014, 346, 1344-1347.	6.0	1,558
59	Accelerating GW calculations with optimal polarizability basis. Physica Status Solidi (B): Basic Research, 2011, 248, 527-536.	0.7	15
60	Fabrication of Polyethylene Superhydrophobic Surfaces by Stretching ontrolled Micromolding. Macromolecular Materials and Engineering, 2009, 294, 295-300.	1.7	25